

# Stabilization of the Eulerian model for incompressible multiphase flow by artificial diffusion

A.W. Vreman

*AkzoNobel, Research Development & Innovation, Process Technology, P.O. Box 9300, 6800 SB Arnhem, The Netherlands*

---

## Abstract

The commonly used Eulerian or continuum model for incompressible multiphase flow is known to be unstable to perturbations for all wavenumbers, even if viscosity terms are used in the momentum equations. In the present work the model is stabilized by adding explicit artificial diffusion to the mass equations. The artificial diffusion terms lead to improved stability properties: uniform flow becomes linearly stable for large wavenumbers, and above an analytically derived threshold for the artificial diffusivity, stability for all wavenumbers is achieved. The artificial diffusivity reappears in the momentum equations, in such a way that fundamental properties of the standard equations remain valid: Galilean invariance is maintained, total mass and momentum are conserved, decay of total kinetic energy is ensured in the absence of external forces, and a flow initially at rest at hydrostatic pressure remains unchanged, even if the spatial distribution of volume fractions is nonuniform. A staggered finite volume pressure correction method using central differencing (leading to energy conserving discretization of convective and pressure terms) is presented. Application of the method to one-dimensional two-phase flow of falling particles confirms that the equations are stable with and unstable without artificial diffusion in the volume fraction equation.

*Keywords:* multiphase flow, multicomponent flow, stability, artificial diffusion, staggered pressure correction methods

---

## 1. Introduction

In the modeling of multiphase flows in the chemical industry the so-called Eulerian model plays an important role [1, 6, 9, 13, 16, 32]. In multiphase flow terminology the word Eulerian is not opposed to viscous but to Lagrangian; it means that the model is a continuum model with different velocities assigned to each phase. The Eulerian model can be distinguished from models that describe the flow in more detail, such as the Euler-Lagrange model (which includes a Lagrangian tracking of all particles in the flow [32]), and immersed boundary methods (which resolve the interfacial surface [27]). The detailed models are important from a fundamental point of view, but most industrial flows cannot yet be simulated by these models, because of the prohibitive computational costs. Therefore the Eulerian model is expected to remain important for quite some time.

---

*Email address:* bert.vreman@akzonobel.com; bert@vremanresearch.nl (A.W. Vreman)

To perform a robust multiphase simulation with the standard Eulerian model is usually not straightforward. Even if the multiphase flow is expected to be statistically stationary, Reynolds averaged Eulerian models frequently require to be run in the transient mode, for convergence reasons. Also dependency of results on the grid can be a problem [19, 12]. These practical problems are likely to be related to the longstanding issue of the linear instability of the basic Eulerian model to perturbations for all wavenumbers. Although the inclusion of viscous terms in the momentum equations in the incompressible case helps, it is not a real solution; it diminishes the unstable growth rates, but does not kill them, not even at infinitely large wavenumber [2, 26, 34]. This also means that the Reynolds averaged equations equipped with a closure model with turbulent eddy-viscosities do not have a stable steady state. As a consequence the equations cannot be used to predict the statistically stationary state of the multiphase flow by means of a steady-state computation, although such a state in many cases seems to be physically well-defined.

The emerging instabilities may be interpreted as Kelvin-Helmholtz instabilities [29, 15]. However, physical Kelvin-Helmholtz instabilities vanish above a critical wavenumber. For example, the critical wavenumber of Kelvin Helmholtz instabilities of an inviscid single-phase free shear layer (two adjacent infinite streams of different velocity) is reversely proportional to the finite thickness of the shear layer [22], and the critical wavenumber reduces for increasing viscosity. But if such a flow is modelled with the one-dimensional two-phase Eulerian model with equal densities of the phases, an infinitely large critical wavenumber is predicted. The underlying assumption of the standard Eulerian model seems to be that a velocity difference between the phases induces infinitely thin free shear layers.

To stabilize the Eulerian model, a number of extensions have been proposed in literature:

1. Inclusion of surface tension through a third order derivative of the volume fraction in the momentum leads to stability at large wavenumbers [29].
2. Inclusion of added mass stabilizes the equations, but only if the volume fraction of the dispersed phase is very small or the added mass coefficient is unrealistically large [7, 18].
3. Inclusion of the gradient of the volume fraction into the momentum equations can also stabilize the equations, but only if the coefficient in front of this term exceeds a certain threshold. The presence of the volume gradient term in the momentum equations can be physically justified by Brownian motion [28], interparticle collisions [32], interfacial pressure differences [24], or turbulent dispersion forces [14, 23, 20, 8]. However, when these effects are small the threshold is not reached and instability still prevails for all wavenumbers.
4. Inclusion of compressibility in combination with (turbulent) viscosity in one or both momentum equations leads to stability at large wavenumbers [2].
5. In compressible cases, the use of multiple pressures (and an extra equation for one of the volume fractions with a right-hand side proportional to the pressure difference between the phases) [3, 4, 25] stabilizes large wavenumber perturbations. In the case of incompressible flow this option is equivalent to adding a bulk viscosity in the momentum equations [34]. Therefore this approach does not stabilize the incompressible equations.

Unfortunately, none of the physical extensions effects in the list above is able to stabilize the multiphase flow equations in basic conditions, i.e. in cases where the particle force is well described by algebraic drag and where surface tension, interparticle collisions, and compressibility are unimportant. Furthermore, laminar or turbulent viscosity terms in the momentum equations are unable to stabilize the equations, no matter how large the viscosities are. However, in numerical simulations some mechanism to regularize instabilities at infinitely short wavelength should be present, otherwise these simulations simply blow up.

For this reason upwind methods, which introduce implicit diffusion, are widely used to discretize the volume fraction equations. But nevertheless, the precise effect of numerical diffusion in the volume fraction equations on stability of the standard Eulerian model is still unknown. Instead of implicit numerical diffusion, one may could also add explicit artificial diffusion terms in the volume fraction equations [12] (see also Refs. [10, 14]). The addition of explicit artificial smoothing terms, including artificial diffusion in the mass equation, is a well-known technique to capture shocks in single-phase compressible flow (see e.g. Ref. [17]). In fact there is no fundamental difference between the use of implicit or explicit artificial diffusion. Recently, Holmas *et al.* [12] investigated a particular 1D two-phase model and showed that with explicit artificial diffusion in the volume fraction equation the model was stable for large wavenumbers. However, that particular model differed from the standard 1D two-phase model in the sense that it contained only two partial differential equations instead of four, and that the state vector contained only two variables (volume fraction and liquid velocity) instead of four (volume fraction, pressure and two velocities). Furthermore, there is no analytical expression for stability at all wavenumbers in Ref. [12].

The purpose of the present work is to investigate the influence of addition of explicit artificial diffusion (second order derivatives of the volume fraction in the mass conservation equations) on the stability of the standard Eulerian multiphase model. Compared to the implicit diffusion introduced by upwind methods, explicit artificial diffusion has the advantage that its control is relatively simple; a modification of the amount of diffusion is straightforward.

The contents of the present paper is as follows. The equations supplemented with artificial diffusion are presented in section 2. The construction of the diffusion terms is such that a number of desirable fundamental properties of the original equations are maintained. In section 3, it is proven that the additional diffusion causes linear stability of uniform two-phase flow for perturbations at large wavenumber. Furthermore, a lower bound for the diffusivity is derived, above which the steady state solution is stable to perturbations of all wavenumbers. Numerical examples for one dimensional flow of falling particles will be presented in section 4, to illustrate the stable behavior caused by the artificial diffusion terms. Conclusions can be found in section 5.

## 2. Equations with artificial diffusion

The basic Eulerian model for incompressible flow of  $N$  phases or components has the following form [1, 6, 9, 13, 16]:

$$\begin{aligned}\partial_t(\rho_n\alpha_n) &= -\partial_j(\rho_n\alpha_n u_{nj}), \\ \partial_j(\rho_n\alpha_n u_n) &= -\partial_j(\rho_n\alpha_n u_{ni}u_{nj}) - \alpha_n\partial_i p + \rho_n\alpha_n g_i\end{aligned}\tag{1}$$

$$+\partial_j(2\alpha_n\rho_n\nu_n S_{ij}) + \gamma_{nm}\alpha_n\alpha_m(u_{mi} - u_{ni}), \quad (2)$$

$$\sum_{n=1}^N \alpha_n = 1. \quad (3)$$

The equations above are imposed on each phase  $n$  (where the phase index  $n$  attains the integer values from 1 to  $N$ ). The volume fraction of phase  $n$  is denoted by  $\alpha_n$ , while  $u_{ni}$  is the velocity component of phase  $n$  in the  $i$ -direction,  $g_i$  the gravity acceleration in the  $i$ -direction,  $\nu_n$  is the sum of molecular and turbulent viscosity of phase  $n$ , and  $S_{nij}$  the  $i, j$  component of the rate of strain tensor viscous stress tensor of phase  $n$ ,  $S_{nij} = \frac{1}{2}(\partial_j u_{ni} + \partial_i u_{nj} - \frac{2}{3}\delta_{ij}\partial_l u_{nl})$ . Since incompressible flow is considered, the material density of each phase ( $\rho_n$ ) is constant. The Einstein summation convention over repeated indices in products is applied to indices  $j$  and  $m$ , but not to indices  $i$  and  $n$ , unless mentioned otherwise. The symbols  $\partial_t$  and  $\partial_j$  denote the differentiations  $\partial/\partial t$  and  $\partial/\partial x_j$ , where  $t$  is time and  $x_j$  the spatial coordinate in direction  $j$ . In addition  $\gamma_{nm}$  is the dimensional drag coefficient [ $\text{kg}/\text{m}^3\text{s}$ ] for the drag between phases  $n$  and  $m$ :  $\gamma_{nm} = \gamma_{mn} \geq 0$  and  $\gamma_{nn} = 0$ . The multiplication of the drag correlation in the momentum equations with  $\alpha_n\alpha_m$  instead of  $\alpha_m$ , is not uncommon in engineering sciences, see e.g. Refs. [30, 31], and is convenient for the linear stability analysis in the next section. For two-phase flow with a dilute second phase  $\alpha_2$  is small, and  $\alpha_1\alpha_2\gamma_{12}$  and  $\alpha_2\gamma_{12}$  are approximately the same.

For two phases the equations above have been implemented in a number of commercial flow packages widely used in industry (see the documentation of the packages). The continuity equations do not contain physical diffusion terms, but the numerical implementation of these equations always require diffusion, and even then instabilities are hard to control. The numerical diffusion is usually implicitly provided, by upwind schemes. In this work we add explicit diffusion terms to the equations, since we wish to investigate the effect of numerical diffusion using analytical tools, and we wish to be able to control the magnitude of numerical diffusion in a direct way.

After the inclusion of artificial diffusion terms, the Eulerian equations for multiphase flow read:

$$\partial_t(\rho_n\alpha_n) = -\partial_j(\rho_n\alpha_n u_{nj}) + \partial_j(\rho_n\eta_n\partial_j\alpha_n), \quad (4)$$

$$\begin{aligned} \partial_t(\rho_n\alpha_n u_{ni}) &= -\partial_j(\rho_n\alpha_n u_{ni}u_{nj}) - \alpha_n\partial_i p + \rho_n\alpha_n g_i \\ &\quad + \partial_j(2\rho_n\alpha_n\nu_n S_{nij}) + \partial_j(u_{ni}\rho_n\eta_n\partial_j\alpha_n) + \gamma_{nm}\alpha_n\alpha_m(u_{mi} - u_{ni}), \end{aligned} \quad (5)$$

$$\sum_{n=1}^N \alpha_n = 1. \quad (6)$$

The variable  $\eta_n$  denotes the artificial diffusivity of phase  $n$  and appears in the volume fraction and momentum equations. It is stressed that the terms with  $\eta_n$  do not have a physical meaning but only serve a numerical purpose. Since the terms with  $\eta_n$  are second-order derivatives, their damping effect on large scales is much weaker than on small scales.

With the definition of modified velocities,

$$w_{nj} = u_{nj} - \eta_n\partial_j\alpha_n, \quad (7)$$

the system expressed by Eqs. (4-6) is equivalent to

$$\partial_t(\rho_n\alpha_n) = -\partial_j(\rho_n\alpha_n w_{nj}), \quad (8)$$

$$\begin{aligned}\partial_t(\rho_n \alpha_n u_{ni}) &= -\partial_j(\rho_n \alpha_n u_{ni} w_{nj}) - \alpha_n \partial_i p + \rho_n \alpha_n g_i \\ &\quad + \partial_j(2\rho_n \alpha_n \nu_n S_{nij}) + \gamma_{nm} \alpha_n \alpha_m (u_{mi} - u_{ni}),\end{aligned}\tag{9}$$

$$\sum_{n=1}^N \alpha_n = 1.\tag{10}$$

This shows that the system with artificial diffusion differs from the standard system (1-3) only in the sense that the convective velocity  $u_{nj}$  in the convective terms has been replaced by  $w_{nj}$ .

In the remainder of this section we will show that (4-6) fulfills four desirable basic properties (see the list of properties in Ref. [34]). The first property is that the system is Galilean invariant, i.e. the equations are invariant under the coordinate transformation  $u_{ni}^* = u_{ni} + U_i$ ,  $x_i^* = x_i + U_i t$  and  $t^* = t$ , where  $U_i$  is constant. This property is recognized if we rewrite Eqs. (4-6) as:

$$\partial_t \alpha_n + u_{nj} \partial_j \alpha_n = -\alpha_n \partial_j u_{nj} + \partial_j(\eta_n \partial_j \alpha_n),\tag{11}$$

$$\begin{aligned}\rho_n \alpha_n \partial_t u_{ni} + \rho_n \alpha_n u_{nj} \partial_j u_{ni} &= -\alpha_n \partial_i p + \rho_n \alpha_n g_i + \partial_j(2\rho_n \alpha_n \nu_n S_{nij}) \\ &\quad + \rho_n \eta_n (\partial_j \alpha_n) (\partial_j u_{ni}) + \gamma_{nm} \alpha_n \alpha_m (u_{mi} - u_{ni}),\end{aligned}\tag{12}$$

$$\sum_{n=1}^N \alpha_n = 1.\tag{13}$$

Since the left-hand sides of Eqs. (11-12) are proportional to material derivatives, and all velocity dependent terms in the right-hand side do only depend on velocity differences or spatial velocity derivatives, the system is Galilean invariant. Of course the artificial diffusivity and viscosities should then also be specified as Galilean invariant expressions.

Provided the artificial diffusivities  $\eta_n$  vanish for zero velocities, system (4-6) has a second property: a flow initially in rest undergoes no change if the pressure is hydrostatic, even if the distribution of phases is nonuniform. This is a desirable property for dispersed multiphase flows, where the effect of Brownian motion is usually negligible [27]. It sufficient to require that the artificial diffusivity vanishes at rest. For zero artificial diffusivity all terms that depend on the derivatives of the volume fractions vanish in Eqs. (11-13). As a consequence, time derivatives remain zero at zero velocities and hydrostatic pressure, even if the volume fractions vary in space. The artificial diffusivity used in section 4 vanishes for zero velocities indeed.

The third property is that the mass and momentum equations summed over the phases are in divergence form, and thus mass and momentum in the averaged variables are conserved with appropriate boundary conditions.

The fourth desirable property is that the total kinetic energy in the averaged variables in the entire volume is guaranteed to reduce with suitable boundary conditions and in the absence of external forces. This property can be derived if the artificial diffusivities in the volume fraction equations are the same, say  $\eta_n = \eta$ . This property, and the previous one, are quite attractive from a practical point of view, because the conservation of quantities and boundedness of kinetic energy are important issues in the development of robust numerical models. The equation for the kinetic energy in the averaged variables can be obtained from the identity

$$\partial_t \left( \frac{1}{2} \rho_n \alpha_n u_{ni} u_{ni} \right) = u_{ni} \partial_t (\rho_n \alpha_n u_{ni}) - \frac{1}{2} u_{ni} u_{ni} \partial_t (\rho_n \alpha_n).\tag{14}$$

In this equation and also in Eqs. (15-18), the summation convention over repeated indices in products is not only applied to the indices  $j$  and  $m$ , but also to the indices  $i$  and  $n$ , in contrast to the equations up to Eq. (13). Substitution of Eqs. (8) and (9) into Eq. (14) leads to

$$\begin{aligned} \partial_t(\frac{1}{2}\rho_n\alpha_n u_{ni}u_{ni}) &= -\partial_j(\frac{1}{2}\rho_n\alpha_n u_{ni}u_{ni}w_{nj} - \alpha_n p u_{nj} + 2\rho_n\alpha_n\nu_n S_{nij}u_{ni}) \\ &\quad + p\partial_i(\alpha_n u_{ni}) - 2\rho_n\alpha_n\nu_n S_{nij}S_{nij} \\ &\quad + \rho_n\alpha_n u_{ni}g_i - \frac{1}{2}\gamma_{nm}\alpha_n\alpha_m(u_{mi} - u_{ni})(u_{mi} - u_{ni}). \end{aligned} \quad (15)$$

For  $\eta_n = \eta$  the sum of the volume fraction equations specified by (4) can be written as:

$$\partial_t \sum_{n=1}^N \alpha_n = -\partial_j(\alpha_n u_{nj}) + \partial_j(\eta\partial_j \sum_{n=1}^N \alpha_n), \quad (16)$$

which is equivalent to

$$\partial_j(\alpha_n u_{nj}) = 0, \quad (17)$$

because the sum of the volume fractions equals 1. Substitution of the latter equation into (15), integration of (15) over the domain  $V$ , absence of body forces ( $g_i = 0$ ), and the application of appropriate boundary conditions (zero normal velocity or periodicity) shows that the total kinetic energy remains bounded,

$$\partial_t \int_V \frac{1}{2}\rho_n\alpha_n u_{ni}u_{ni}dV = - \int_V (2\rho_n\alpha_n\nu_n S_{nij}^2 + \frac{1}{2}\gamma_{nm}\alpha_n\alpha_m(u_{mi} - u_{ni})^2) \leq 0, \quad (18)$$

provided the viscosities  $\nu_n$  and the averaged drag coefficients  $\gamma_{nm}$  are positive.

### 3. Linear stability

In this section we will consider the linear stability of the equations formulated in the previous section. The analysis will be focussed on the linear stability of uniform one-dimensional two-phase flow. As mentioned in the Introduction, for this relatively simple flow the standard model without artificial diffusion is known to be linearly unstable to perturbations for all wavenumbers, even if viscous terms are incorporated into the momentum equation.

We start with some remarks on assumptions and notation for the cases of one-dimensional two-phase flow considered in this and the following section. The factor  $2/3$  in the definition of the strainrate  $S_{ij}$  is replaced by 1. Furthermore, the indices  $i$  and  $j$  are omitted and the spatial derivative is denoted with  $\partial_x$ . We take a single artificial diffusivity  $\eta_1 = \eta_2 = \eta$  and the single dimensional drag coefficient is denoted with  $\gamma$ . Thus the equations that will be analyzed are (compare Eqs. (11-12)):

$$\partial_t\alpha_1 + u_1\partial_x\alpha_1 + \alpha_1\partial_x u_1 - \partial_x(\eta\partial_x\alpha_1) = 0, \quad (19)$$

$$-\partial_t\alpha_1 - u_2\partial_x\alpha_1 + \alpha_2\partial_x u_2 + \partial_x(\eta\partial_x\alpha_1) = 0, \quad (20)$$

$$\begin{aligned} \partial_t u_1 + u_1\partial_x u_1 + \frac{1}{\rho_1}\partial_x p - g - \frac{1}{\alpha_1}\partial_x(\alpha_1\nu_1\partial_x u_1) \\ - \eta(\partial_x\alpha_1)(\partial_x u_1) - \frac{\gamma\alpha_2}{\rho_1}(u_2 - u_1) = 0, \end{aligned} \quad (21)$$

$$\begin{aligned} \partial_t u_2 + u_2\partial_x u_2 + \frac{1}{\rho_2}\partial_x p - g - \frac{1}{\alpha_2}\partial_x(\alpha_2\nu_2\partial_x u_2) \\ - \eta(\partial_x\alpha_2)(\partial_x u_2) + \frac{\gamma\alpha_1}{\rho_2}(u_2 - u_1) = 0, \end{aligned} \quad (22)$$

and  $\alpha_2 = 1 - \alpha_1$ . Here  $\eta$  and  $\nu_1$  and  $\nu_2$  are allowed to be functions of the field variables  $\alpha_1$ ,  $\alpha_2 = 1 - \alpha_1$ ,  $u_1$  and  $u_2$ . The drag coefficient  $\gamma$  is allowed to be a function of the relative velocity  $u_2 - u_1$ .

In the remainder of this section (but not in the following section) the symbols  $\alpha_1$ ,  $\alpha_2 = 1 - \alpha_1$ ,  $u_1$ ,  $u_2$ , and  $p$  will represent the non-fluctuating uniform field for which the stability is investigated ( $\alpha_1$ ,  $\alpha_2$ ,  $u_1$  and  $u_2$  are constant in time and space,  $p$  is constant in time and linear in space). Likewise  $\eta$ ,  $\nu_1$ ,  $\nu_2$  will represent the non-fluctuating part of the artificial diffusivity and (turbulent) viscosities. It is remarked that the fluctuating parts of the diffusivity and viscosities do not play a role in a linear analysis, since they only appear in terms that are products of fluctuations (diffusivity and viscosities are multiplied with derivatives of volume fraction or velocities and the non-fluctuating parts of these derivatives are zero). However, the fluctuating part of the drag will affect the linear analysis. For this purpose, we define

$$\hat{\gamma} = \frac{\partial(u_2 - u_1)\gamma}{\partial(u_2 - u_1)} = \gamma + (u_2 - u_1)\frac{\partial\gamma}{\partial(u_2 - u_1)}, \quad (23)$$

and in the remainder of this section  $\hat{\gamma}$  will represent the non-fluctuating part of this variable.

As is common in linear stability analyses we assume a perturbation vector proportional to

$$\exp(i\omega t - ikx), \quad (24)$$

and superimpose it on the uniform field. Here  $k$  is the real spatial wavenumber ( $k > 0$ ),  $\omega$  is a complex number and  $i^2 = -1$  ( $i$  does not represent an index in this section). The real part of  $\omega$  represents the propagating velocity of the wave. The growth rate is defined by

$$\Omega = -\text{Im}(\omega). \quad (25)$$

A negative, zero or positive growth rate corresponds to a stable, neutral or unstable wave, respectively.

If we substitute the uniform field plus the Fourier perturbation into Eqs. (11-13), linearize by omitting terms containing products of fluctuations, use the property that derivatives of the constant field are zero, and divide the resulting equations by  $ik \exp(i\omega t - ikx)$ , then we obtain a system of linear equations for the amplitudes of the perturbation. The linear system represents a degenerate eigenvalue problem, and a nontrivial solution for the vector with amplitudes exists if the following determinant is zero:

$$\begin{vmatrix} \frac{\omega}{k} - u_1 - i\eta k & -\alpha_1 & 0 & 0 \\ u_2 + i\eta k - \frac{\omega}{k} & 0 & -\alpha_2 & 0 \\ \frac{i\gamma(u_1 - u_2)}{\rho_1 k} & \frac{\omega}{k} - u_1 - i\nu_1 k - \frac{i\hat{\gamma}\alpha_2}{\rho_1 k} & \frac{i\hat{\gamma}\alpha_2}{\rho_1 k} & -\frac{1}{\rho_1} \\ \frac{i\gamma(u_1 - u_2)}{\rho_2 k} & \frac{i\hat{\gamma}\alpha_1}{\rho_2 k} & \frac{\omega}{k} - u_2 - i\nu_2 k - \frac{i\hat{\gamma}\alpha_1}{\rho_2 k} & -\frac{1}{\rho_2} \end{vmatrix} = 0, \quad (26)$$

where  $\alpha_2 = 1 - \alpha_1$ . The four rows in the determinant correspond to the four equations above, while the columns correspond to the perturbation superimposed on the variables  $\alpha_1$ ,  $u_1$ ,  $u_2$ ,  $p$ , respectively.

It appears to be convenient to define eigenvalues with the dimension of velocity by:

$$\lambda = \frac{\omega}{k} - i\eta k, \quad (27)$$

and to use separate symbols  $s$  and  $y$  for the real and imaginary parts of  $\lambda$ , i.e.

$$\lambda = s + iy. \quad (28)$$

This implies that the growth rate  $\Omega$  of the perturbation wave equals

$$\Omega = -\text{Im}(\omega) = -\text{Im}(\lambda)k - \eta k^2 = -yk - \eta k^2. \quad (29)$$

Substitution of definition (27) into Eq. (26) and expansion of the determinant (see Appendix 1) leads to the quadratic polynomial

$$a\lambda^2 - (b + iq)\lambda + c + ir = 0, \quad (30)$$

where

$$a = \alpha_2\rho_1 + \alpha_1\rho_2, \quad (31)$$

$$b = 2(\alpha_2\rho_1u_1 + \alpha_1\rho_2u_2), \quad (32)$$

$$c = \alpha_2\rho_1u_1^2 + \alpha_1\rho_2u_2^2, \quad (33)$$

$$q = \frac{\hat{\gamma}}{k} + k(\alpha_2\rho_1(\nu_1 - \eta) + \alpha_1\rho_2(\nu_2 - \eta)), \quad (34)$$

$$r = \frac{\hat{\gamma}}{k}w + k(\alpha_2\rho_1(\nu_1 - \eta)u_1 + \alpha_1\rho_2(\nu_2 - \eta)u_2), \quad (35)$$

$$w = \alpha_1u_2 + \alpha_2u_1. \quad (36)$$

Substitution of  $\lambda = s + iy$  into Eq. (30) leads to

$$ay^2 - qy - as^2 + bs - c = 0, \quad (37)$$

$$(2as - b)y - qs + r = 0. \quad (38)$$

From equation (37) we solve  $y$ :

$$y = \frac{q \pm (q^2 + 4a(as^2 - bs + c))^{\frac{1}{2}}}{2a}. \quad (39)$$

The classic inviscid case without drag is recovered if  $\eta = 0$ ,  $\nu_{1,2} = 0$  and  $\hat{\gamma} = 0$ . Then  $q$  and  $r$  are zero and the roots  $\lambda$  of Eq. (30) are the standard complex characteristic velocities [9, 21, 27, 29]:

$$\lambda = \frac{\alpha_2\rho_1u_1 + \alpha_1\rho_2u_2 \pm i|u_1 - u_2|(\alpha_1\alpha_2\rho_1\rho_2)^{\frac{1}{2}}}{\alpha_2\rho_1 + \alpha_1\rho_2}. \quad (40)$$

The occurrence of complex roots implies that there is an unstable growth rate ( $\Omega > 0$ ) for all wavenumbers  $k \neq 0$  in case  $u_1 \neq u_2$ . It also implies that for zero  $q$  and  $r$  the left-hand side of Eq. (30) is positive definite in real space; hence

$$as^2 - bs + c > 0 \quad (41)$$

for all  $s$  and  $u_1 \neq u_2$ .

The focus of the present section is on stability, but before we proceed with the stability analysis, we discuss the related concepts well-posedness, hyperbolicity and wave

dispersion. Because the classic inviscid Eulerian model has complex characteristic velocities (Eq. (40)), it is ill-posed. The characteristic velocity is in fact the quantity  $\omega/k$ , provided  $\omega/k$  does not depend on  $k$  [36]. If there are  $N$  real characteristic velocities for a system of rank  $N$ , the linear system is purely hyperbolic. Such systems are known to be well-posed, that is for appropriate initial and boundary conditions a unique solution exists and the dependence of this solution on the initial and boundary data is continuous. If  $\omega/k$  is real but not constant, the system is not hyperbolic but dispersive ([36], p365). Since characteristic velocities are roots of a polynomial with real coefficients, complex characteristic velocities always appear as complex conjugate pairs. This implies that systems with complex characteristic velocities are unstable. Even if the classic inviscid system had two real characteristic velocities it would not be strictly hyperbolic because the rank of the system is four, while the rank of the characteristic polynomial is only two (the eigenvalue problem is called degenerated). This is due to the elliptic behavior arising from the role of pressure in incompressible flow. In the present work we include the effects of diffusion, viscosity and drag, which adds parabolic features to the system. Since  $\omega/k$  depends on  $k$ , there are no characteristic velocities anymore. In addition  $\omega/k$  is complex but does not appear in complex conjugate pairs, which means that complex roots do not necessarily imply instability; if the imaginary parts of all solutions  $\omega/k$  are positive the system is stable. Although formal analysis of dispersion requires  $\omega/k$  to be real [36], information on dispersive behavior may be extracted from the propagation velocity  $s$ , the real part of  $\omega/k$ , which also depends on  $k$ .

We next proceed with the linear instability analysis and include the effects of the artificial diffusivity, viscosities and drag. This means that the coefficients  $q$  and  $r$  are in general nonzero. The definition of  $q$  (34) shows that the limit  $|q| \rightarrow \infty$  is important for the behavior of the system at small and large wavenumbers. For  $|q| \rightarrow \infty$  and finite  $s$  the Taylor expansion applied to (39) indicates that the asymptotic limit of one root is given by

$$y \rightarrow q/a \rightarrow -\eta k + (\alpha_2 \rho_1 \nu_1 + \alpha_1 \rho_2 \nu_2) \frac{k}{a}. \quad (42)$$

Substitution of  $y \rightarrow q/a$  into Eq. (38) shows that the corresponding propagation velocity  $s$  converges to  $b/a - r/q$ , which is finite indeed. The asymptotic limit ( $|q| \rightarrow \infty$ ) of the other root is given by

$$y \rightarrow -\frac{as^2 - bs + c}{q}. \quad (43)$$

Equation (43) shows that  $|q| \rightarrow \infty$  implies  $y \rightarrow 0$ ; hence from equation (38) it can be verified that  $s \rightarrow r/q$ , which is finite indeed. The maximum asymptotic growth rate is obtained from the substitution of (42) and (43) into (29):

$$\Omega_{max} = \max\left(-(\alpha_2 \rho_1 \nu_1 + \alpha_1 \rho_2 \nu_2) \frac{k^2}{a}, (as^2 - bs + c) \frac{k}{q} - \eta k^2\right). \quad (44)$$

The multiphase equations with viscosity and drag but without artificial diffusion are retrieved if  $\nu_{1,2} > 0$ ,  $\hat{\gamma} > 0$  and  $\eta = 0$ . In this case  $k \rightarrow \infty$  implies  $q \rightarrow +\infty$ . Thus the maximum asymptotic growth rate  $\Omega_{max}$  given by Eq. (44) reduces to

$$\frac{as^2 - bs + c}{\alpha_2 \rho_1 \nu_1 + \alpha_1 \rho_2 \nu_2}, \quad (45)$$

which is a positive constant, positive because of (41). Thus there is a serious instability for perturbations at large wavenumber if  $\eta = 0$ , which is not removed by the viscosity in the momentum equations [2, 26, 34].

In the following the stabilizing effect of nonzero diffusivity in the volume fraction equation will be analyzed ( $\eta > 0$ ,  $\hat{\gamma} > 0$ ,  $\nu_1 > 0$ ,  $\nu_2 \geq 0$ ). The results will be presented in three parts: stability for large wavenumbers, stability for small wavenumbers, and stability for all wavenumbers.

First, we consider the large wavenumber limit,  $k \rightarrow \infty$ . To investigate this limit, we define  $\zeta$  by

$$\zeta = \alpha_2 \rho_1 (\nu_1 - \eta) + \alpha_1 \rho_2 (\nu_2 - \eta). \quad (46)$$

If  $\zeta \neq 0$  then  $k \rightarrow \infty$  implies  $|q| \rightarrow \infty$ . Thus Eq. (44) is applicable, which implies that that the system is stable in the large wavenumber limit;  $\eta > 0$  implies  $\Omega_{max} \sim -k^2 \rightarrow -\infty$ . If  $\zeta = 0$  then  $k \rightarrow \infty$  implies  $q \rightarrow 0$  and either  $r \rightarrow 0$  or  $|r| \rightarrow \infty$ . If  $q \rightarrow 0$  and  $r \rightarrow 0$ , the roots  $\lambda$  converge to the roots given by Eq. (40). Substitution of Eq. (40) into Eq. (27) implies that  $\Omega$  has a negative imaginary part for  $k \rightarrow \infty$ . In Appendix 1 it is shown that  $\Omega$  has also a negative imaginary part if  $q \rightarrow 0$  and  $|r| \rightarrow \infty$ . Hereby the proof is finished that the system is stable for large wavenumbers if  $\eta > 0$ ,  $\hat{\gamma} > 0$ ,  $\nu_1 > 0$ , and  $\nu_2 \geq 0$ .

For the special case  $\hat{\gamma} = 0$  and  $\eta = \nu_1 = \nu_2$ , the parameters  $q$  and  $r$  are zero. Since  $\lambda$  then converges to Eq. (40), it is straightforward to find the critical wave number  $k_{crit}$ , above which the equations are stable. The critical wavenumber is reached if one solution for  $\Omega$  is zero (and the other one negative). Eqs. (29) and (40) imply that

$$k_{crit} = \frac{(\alpha_1 \alpha_2 \rho_1 \rho_2)^{\frac{1}{2}} |u_1 - u_2|}{\eta (\alpha_2 \rho_1 + \alpha_1 \rho_2)}. \quad (47)$$

It is remarked that for sufficiently large  $k_{crit}$  the effect of nonzero  $\hat{\gamma}$  on  $k_{crit}$  will be small, since unlike viscous terms the effect of the drag term does not increase with  $k$ , because the term is algebraic. Using the Nyquist relation  $k_{crit} = 2\pi/L$ , Eq. (47) is rewritten to obtain the value of the diffusion coefficient that damps out unstable waves that are shorter than some sufficiently small length-scale  $L$ :

$$\eta = \frac{(\alpha_1 \alpha_2 \rho_1 \rho_2)^{\frac{1}{2}} |u_1 - u_2| L}{2\pi (\alpha_2 \rho_1 + \alpha_1 \rho_2)}. \quad (48)$$

The latter equation can be useful if the flow displays physical unsteadiness that needs to be computed down to a given length-scale  $L$ . In dispersed multiphase flow  $L$  should not be smaller than the particle diameter.

Second, we derive a constraint for  $\eta$  for which stability in the small wavenumber limit is ensured. The limit  $k \rightarrow 0$  implies  $q \rightarrow +\infty$ . The potential unstable root is then given by Eq. (43), which implies  $y \rightarrow 0$ , and as a consequence the asymptotic propagation velocity, deduced from (38), equals

$$s = \frac{r}{q} = w. \quad (49)$$

Substitution into (43) leads to

$$y = -\frac{aw^2 - bw + c}{\hat{\gamma}/k}. \quad (50)$$

Since

$$aw^2 - bw + c = (u_1 - u_2)^2 \alpha_1 \alpha_2 (\alpha_1 \rho_1 + \alpha_2 \rho_2) \quad (51)$$

(see Appendix 1), it follows from the definitions of  $a$ ,  $b$ ,  $c$  and  $w$  that

$$y = -\frac{k}{\hat{\gamma}} (u_1 - u_2)^2 \alpha_1 \alpha_2 (\alpha_1 \rho_1 + \alpha_2 \rho_2) \quad (52)$$

for  $k \rightarrow 0$ . Hence perturbations at small wavenumbers (large wavelengths) are stable if

$$\eta \geq \frac{1}{\hat{\gamma}} (u_1 - u_2)^2 \alpha_1 \alpha_2 (\alpha_1 \rho_1 + \alpha_2 \rho_2), \quad (53)$$

since then the growth rate  $\Omega$  is negative (see definition (29)).

Third, we show that if constraint (53) is fulfilled all wavenumbers are stable. In fact we prove that there is no neutral wave ( $k \neq 0$ ) if the constraint is fulfilled. Since we have already shown that the system is stable for large wavenumbers if  $\eta > 0$ , other wavenumbers can be unstable only if there is a strictly positive wavenumber  $k$  with zero growth rate. Since the system is Galilean invariant we may take any reference velocity; thus without loss of generality we assume  $w = 0$ . In that case Eq. (51) implies that constraint (53) reduces to

$$\eta \hat{\gamma} \geq c. \quad (54)$$

To simplify the analysis further, equal viscosities ( $\nu_1 = \nu_2 > 0$ ) are assumed, denoted with  $\nu$ . Thus Eqs. (34-35) reduce to  $q = \hat{\gamma} + ak(\nu - \eta)$  and  $r = \frac{1}{2}bk(\nu - \eta)$ .

A neutral growth rate  $\Omega$  corresponds to  $y = -\eta k$ . Substitution into Eqs. (37-38) leads to

$$av\eta k^2 + \eta \hat{\gamma} - c - as^2 + bs = 0, \quad (55)$$

$$s = \frac{b(\nu + \eta)k^2}{2\hat{\gamma} + 2a(\nu + \eta)k^2}. \quad (56)$$

Substitution of the latter expression into the former provides

$$(av\eta k^2 + \eta \hat{\gamma} - c)(2\hat{\gamma} + 2a(\nu + \eta)k^2)^2 - ab^2(\nu + \eta)^2 k^4 + b^2(\nu + \eta)k^2(2\hat{\gamma} + 2a(\nu + \eta)k^2) = 0, \quad (57)$$

equivalent to

$$(av\eta k^2 + \eta \hat{\gamma} - c)(2\hat{\gamma} + 2a(\nu + \eta)k^2)^2 + ab^2(\nu + \eta)^2 k^4 + 2\hat{\gamma}b^2(\nu + \eta)k^2 = 0. \quad (58)$$

If constraint (54) is satisfied, Eq. (58) does not have a real solution different from zero. The reason is that  $\eta \hat{\gamma} \geq c$  implies that the left-hand side is strictly positive for  $k \neq 0$  (since  $k^2 > 0$ ,  $a > 0$ ,  $b^2 \geq 0$ ,  $\hat{\gamma} > 0$ ,  $\nu > 0$  and  $\eta \geq 0$ ). In other words stability for all wavenumbers is achieved if  $\eta$  satisfies the constraint Eq. (53). For  $\hat{\gamma} = 0$  the constraint is not satisfied if  $u_1 \neq u_2$ . In this case, the solution of (58), which is the critical wavenumber, can simply be found:

$$k_{crit} = \frac{(\alpha_1 \alpha_2 \rho_1 \rho_2)^{\frac{1}{2}} |u_1 - u_2|}{(\eta \nu)^{\frac{1}{2}} (\alpha_2 \rho_1 + \alpha_1 \rho_2)}, \quad (59)$$

which is a generalization of Eq. (47), since it is also valid for  $\eta \neq \nu$ .

Before we proceed with the next section, we discuss the constraint (53) somewhat more. For the dilute flow, the present dimensional drag coefficient can be written as

$$\gamma = \frac{3C_D}{4d}\rho_1|u_1 - u_2|, \quad (60)$$

where  $C_D$  is the standard dimensionless drag coefficient,  $d$  the spherical particle diameter and  $\rho_1$  the density of the continuous phase. For constant  $C_D$  we have  $\hat{\gamma} = 2\gamma$ , and the stability constraint (53) is then equivalent to

$$\frac{2\alpha_1\alpha_2(\alpha_1 + \alpha_2\frac{\rho_2}{\rho_1})}{3C_D} \left[ \frac{|u_1 - u_2|d}{\eta} \right] \leq 1. \quad (61)$$

The quantity between square brackets is an artificial Peclet number, based on the relative velocity, particle diameter and artificial diffusivity  $\eta$ . For Stokes flow the drag expression above reduces to

$$\gamma = \frac{18\mu_1}{d^2}, \quad (62)$$

where  $\mu_1$  is the dynamic molecular viscosity of the continuous phase. Then  $\hat{\gamma} = \gamma$  and the stability constraint (70) is equivalent to

$$18\alpha_1\alpha_2(\alpha_1 + \alpha_2\frac{\rho_2}{\rho_1}) \left[ \frac{|u_1 - u_2|d}{\mu_1/\rho_1} \right] \left[ \frac{|u_1 - u_2|d}{\eta} \right] \leq 1, \quad (63)$$

which expresses a stability bound on the product of particle Reynolds number (the quotient between the first pair of brackets) and the artificial particle Peclet number.

#### 4. Numerical implementation

In this section we will show examples of implementation for one-dimensional flow of falling particles. First, we will specify the equations presented in section 2 for one-dimensional flow of falling particles. Second, we will specify the numerical scheme, which uses central differencing and pressure correction on a staggered grid. Third, we will show numerical results to illustrate the stability theory of section 3 for falling particles with uniform mean profiles. Fourth, results of simulations of a case with nonuniform mean steady state profiles will be shown.

For two phases, one dimension and equal artificial diffusivities the system of equations given by by Eqs. (4-6) reduces to:

$$\partial_t\alpha_1 = -\partial_x(\alpha_1u_1) + \partial_x(\eta\partial_x\alpha_1), \quad (64)$$

$$\partial_t\alpha_2 = -\partial_x(\alpha_2u_2) + \partial_x(\eta\partial_x\alpha_2), \quad (65)$$

$$\begin{aligned} \partial_t(\alpha_1u_1) &= -\partial_x(\alpha_1u_1^2) - \frac{\alpha_1}{\rho_1}\partial_x p + \alpha_1g \\ &\quad + \partial_x(\alpha_1\nu_1\partial_xu_1) + \partial_x(u_1\eta\partial_x\alpha_1) + \frac{\gamma\alpha_1\alpha_2}{\rho_1}(u_2 - u_1), \end{aligned} \quad (66)$$

$$\begin{aligned} \partial_t(\alpha_2u_2) &= -\partial_x(\alpha_2u_2^2) - \frac{\alpha_2}{\rho_2}\partial_x p + \alpha_2g \\ &\quad + \partial_x(\alpha_2\nu_2\partial_xu_2) + \partial_x(u_2\eta\partial_x\alpha_2) - \frac{\gamma\alpha_1\alpha_2}{\rho_2}(u_2 - u_1), \end{aligned} \quad (67)$$

where  $\alpha_2 = 1 - \alpha_1$ .

The standard drag law is used for  $\gamma$  (see Eq. (60)), where  $C_D$  is provided by the Schiller Naumann empirical correlation,

$$C_D = \frac{24}{Re_p}(1 + 0.15Re_p^{0.687}), \quad (68)$$

if  $Re_p < 1000$ , and otherwise  $C_D = 0.44$ . Here,  $Re_p = \rho_1|u_1 - u_2|d/\mu_1$  is the particle Reynolds number, based upon particle diameter  $d$  and continuous phase molecular viscosity  $\mu_1$ , the continuous phase being denoted with index 1 and dispersed phase with index 2. The drag coefficient (68) implies

$$\gamma = \frac{18\mu_1}{d^2}(1 + 0.15Re_p^{0.687}). \quad (69)$$

The artificial diffusivity is suggested by stability constraint (53),

$$\eta = c_\eta(u_1 - u_2)^2\alpha_1\alpha_2(\alpha_1\rho_1 + \alpha_2\rho_2)/\hat{\gamma}, \quad (70)$$

where  $c_\eta$  is a positive coefficient and according to Eq. (23),

$$\hat{\gamma} = \frac{18\mu_1}{d^2}(1 + 1.687 \cdot 0.15Re_p^{0.687}) \quad (71)$$

if  $Re_p < 1000$ , and  $\hat{\gamma} = 2\gamma$  otherwise. It is remarked that the expression for  $\eta$  is such that the four properties discussed in section 3 section are valid, including the third property on rest states of the flow. If the flow is in rest  $u_1 = u_2$ , and consequently  $\eta = 0$  according to definition (70). This implies that a nonuniform concentration field remains unchanged if the flow is in rest at hydrostatic pressure.

For the numerical solution of these equations, a pressure correction method on a staggered grid, analogous to the standard pressure correction method for incompressible flow [11, 33, 35], is presented for the time-dependent multiphase equations. The volume fractions and pressure are defined in cell centers, and the velocities on cell faces. The spatial discretization is the standard second-order finite volume method, which is based on central differences. Since the first two equations imply

$$\partial_x(\alpha_1u_1 + \alpha_2u_2) = 0, \quad (72)$$

we replace the second continuity equation (65) by a Poisson equation for the pressure,

$$\partial_x\left(\left(\frac{\alpha_1}{\rho_1} + \frac{\alpha_2}{\rho_2}\right)\partial_x p\right) = \partial_x(H_1 + H_2), \quad (73)$$

where  $H_1$  and  $H_2$  are the right-hand sides of (66) and (67) without the pressure gradient terms,

$$H_1 = -\partial_x(\alpha_1u_1^2) + \alpha_1g + \partial_x(\alpha_1\nu_1\partial_xu_1) + \partial_1(u_1\eta\partial_x\alpha_1) + \frac{\gamma\alpha_1\alpha_2}{\rho_1}(u_2 - u_1), \quad (74)$$

$$H_2 = -\partial_x(\alpha_2u_2^2) + \alpha_2g + \partial_x(\alpha_2\nu_2\partial_xu_2) + \partial_2(u_2\eta\partial_x\alpha_2) - \frac{\gamma\alpha_1\alpha_2}{\rho_2}(u_2 - u_1). \quad (75)$$

A time step of the pressure correction method consists out of the six sequential parts:

1. The discretized right-hand side of the first continuity equation (64) is determined. Cell face quantities computed for the  $\alpha_1$ -equations (the sum of convective and diffusive fluxes) are stored for reuse in the computation of  $H_1$ . Also cell face quantities for the  $\alpha_2$  equation are computed and stored such that they can be used when  $H_2$  is computed. This reuse of fluxes through faces also happens in staggered finite volume methods for compressible single-phase flow [5].
2. The terms  $H_1$  and  $H_2$  are computed.
3. Volume fraction  $\alpha_1$  is updated to the new time level using Eq. (64), and  $\alpha_2$  at the new time level is obtained by  $\alpha_2 = 1 - \alpha_1$ .
4. The uncorrected momentum at the new time level is obtained by updating  $\alpha_n u_n$  with  $(\Delta t)H_n$ , where  $\Delta t$  is the time step.
5. The Poisson equation (73) is solved, using lexicographic Gauss-Seidel iteration with overrelaxation factor 1.5.
6. Finally the uncorrected momentum is updated with  $-(\Delta t)\alpha_n \partial_x p$ .

The time discretization is explicit and the forward Euler method is used. Apart from the effects of time discretization, external forces and boundary conditions, the total kinetic energy in the discrete equations cannot increase. This property relies on the energy conserving property of the discretized convective and volume fraction diffusive terms (proven in Appendix 2), and the straightforward skew-symmetry of the spatial derivative operator that appears in Eq. (72), the pressure gradient term and the standard diffusive terms [33].

Results are presented for two types of flows: one with a uniform steady state, another one with a nonuniform steady state. In both cases we consider a flow of particles falling through a continuous phase with density  $\rho_1 = 1.2\text{kg/m}^3$  and molecular viscosity  $\mu_1 = 1.8 \cdot 10^{-5}\text{kg}/(\text{m} \cdot \text{s})$ . The density of the particles equals  $\rho_2 = 1000\text{kg/m}^3$ , their diameter equals  $d = 10^{-3}\text{m}$ , and the gravity acceleration is  $9.8\text{m/s}^2$ . The (turbulent) viscosities are assumed to be equal and constant,  $\nu_1 = \nu_2 = 0.01\text{m}^2/\text{s}$ .

The case with the uniform steady state is simulated in a domain with a length of 1m, using periodic boundary conditions and the initial condition

$$u_1 = u_2 = 0, \tag{76}$$

$$\alpha_2 = 0.1 + 0.05 \sin(2\pi x). \tag{77}$$

The boundary condition for the pressure is obtained from the relation  $p(x+1, t) = p(x, t) + (0.9\rho_1 + 0.1\rho_2)g$ . It can simply be verified that the equations allow the following steady state for this set of boundary and initial conditions:  $\alpha_2 = 0.1$  and  $u_2 - u_1 = 3.87\text{m/s}$ . Three different values for the artificial diffusion coefficient  $c_\eta$  are used: 0, 0.1 and 1. Each of these three cases are performed on two uniform grids, one with 50, the other with 100 cells, corresponding to a mesh size  $h$  of 0.02m and 0.01m, respectively. For these two grids the timestep equals 1 and 0.5 millisecond, respectively.

Results of the six simulations of the case with the uniform steady state are shown in Fig. 1. Fig. 1a shows the maximum fluctuation of the volume fraction,  $\max|\alpha_2 - 0.1|$  as a function of time. Fig. 1b shows the particle slip velocity  $u_2 - u_1$  at  $x = 0$  as a function of time. The results of these simulations are nearly grid independent (see Fig. 1, coarse and fine grid curves almost coincide) The simulations without artificial diffusivity ( $c_\eta = 0$ ) fail. Grid refinement does not remove the instability, due to the fact that the equations

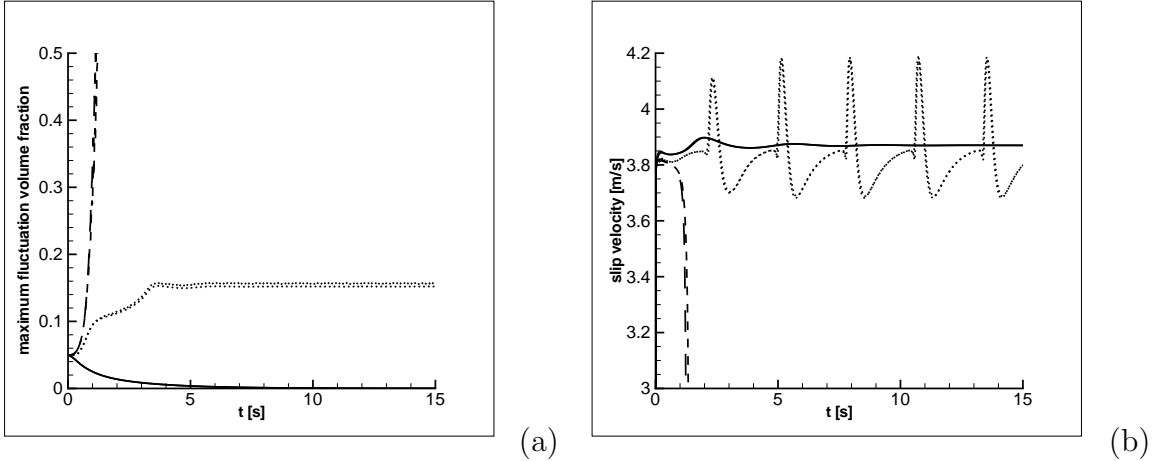


Figure 1: Uniform flow case. Maximum fluctuation of volume fraction (a) and slip velocity at  $x = 0$  (b) as functions of time for  $c_\eta = 0$  (dashed),  $c_\eta = 0.1$  (dotted), and  $c_\eta = 1$  (solid). Results are shown for two different resolutions (curves are approximately on top of each other).

for  $c_\eta = 0$  are unstable for all wavenumbers; after grid refinement the blowup for  $c_\eta$  occurs even slightly earlier. However, the simulations performed with nonzero  $c_\eta$  do not fail, For  $c_\eta = 0.1$  disturbances at large wavenumbers are stable, but disturbances at small wavenumbers are not stable. For this reason the sinusoidal fluctuation in the initial condition does not disappear. Due to nonlinear interactions it saturates after some time, displaying a time-periodic fluctuation of the terminal slip velocity at fixed location (Fig. 1b). In the third case,  $c_\eta = 1$  the linear stability constraint (53) is satisfied. Therefore this simulation is expected to be stable for perturbations at all wavenumbers. Indeed, Fig. 1 shows that in this case the transient solution converges to the steady state solution. From the three values of  $c_\eta$  considered, the simulation with  $c_\eta = 1$  is clearly the most appropriate choice, if we are interested to find the steady state solution of the equations. In the steady state  $\eta = 0.034\text{m}^2/\text{s}$  if  $c_\eta = 1$ .

The present central differencing scheme does not introduce implicit numerical diffusion into the simulations. If the standard first-order upwind method (without explicit artificial diffusion) had been employed, the maximum implicit diffusion would have been  $\max|u_1, u_2|h/2$ , about  $0.04\text{m}^2/\text{s}$  on the coarse and  $0.02\text{m}^2/\text{s}$  on the fine grid. The upwind diffusion decreases with mesh size and upwind simulations without explicit diffusion are therefore expected to develop non-vanishing unsteady oscillations if the mesh size decreases and the implicit diffusion falls below the value prescribed by stability constraint (53). Indeed, two-phase simulations using only implicit (upwind) diffusion were found to diverge with grid refinement [12].

The addition of artificial diffusion with a value of  $\eta$  that satisfies Eq. (53) could lead to additional spreading of physical spatial gradients that may be present in the flow. To address this issue, a second flow case is simulated, this time with a nonuniform steady state. The physical parameters are the same as above, but domain size, boundary

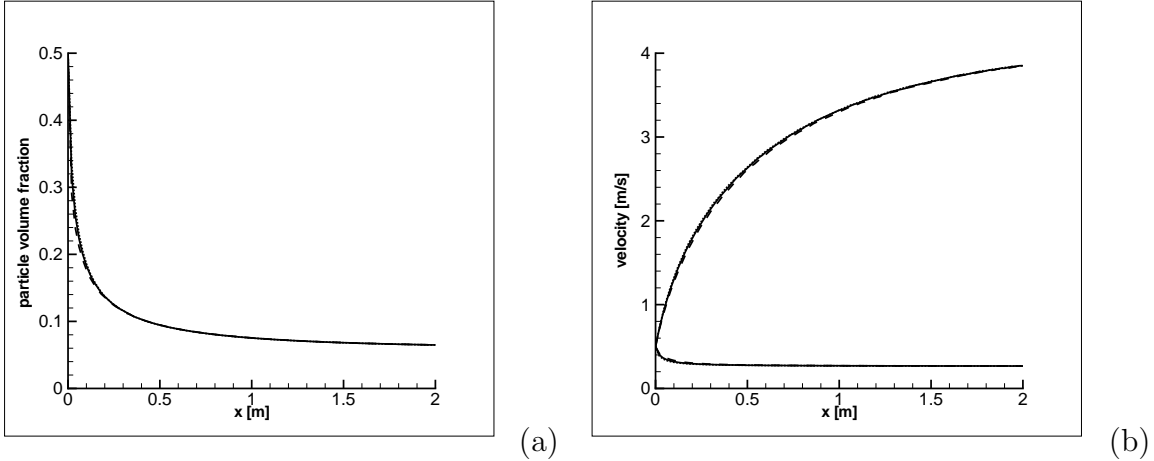


Figure 2: Steady state profiles for the volume fraction  $\alpha_2$  (a), velocity  $u_1$  (b; lower set of curves), and velocity  $u_2$  (b; higher set of curves). Results are shown for three different values of  $c_\eta$ : 0.3 (dotted), 1.0 (solid) and 3.0 (dashed); dotted, solid and dashed curves are approximately on top of each other.

conditions and initial condition are different. The nonuniform case represents a dense flow of particles with relatively low velocity when they start to fall. The length of the domain in this case is 2m, and the inflow boundary conditions are prescribed by  $\alpha_2 = 0.5$ ,  $u_1 = u_2 = 0.5\text{m/s}$ , and zero pressure gradient. The outflow boundary conditions are a fixed pressure and zero gradients for the volume fraction and velocities. The inflow values for volume fraction and velocities are also used as initial condition. A uniform grid of 100 cells is used and the time step is determined by keeping the maximum of the CFL and RK number equal to 0.2.

Results of the computed steady state of the nonuniform flow case are shown in Fig. 2, for three different values of  $c_\eta$ : 0.3, 1 and 3, the largest value being an order of magnitude larger than the smallest one. All three simulations eventually reach the steady state. However,  $c_\eta$  should not be smaller than 0.3, then the simulation of this flow case blows up. The maximum artificial diffusion in the steady state equals 0.005, 0.016 and  $0.046\text{m}^2/\text{s}$  for  $c_\eta=0.3, 1$  and 3, respectively. Fig. 2 shows that the profiles of  $c_\eta=0.3, 1$  and 3 are nearly identical. It is concluded that the effect of the artificial diffusion term on the spreading of the mean gradients is small.

## 5. Conclusions

The commonly used Eulerian or continuum model for incompressible multiphase flow is known to be unstable to perturbations for all wavenumbers, even if (turbulent) viscosities are used in the momentum equations. In the present work the model was stabilized by the addition of artificial diffusion in the form of second order derivatives of the concentrations in the mass and momentum equation. The artificial diffusion terms were shown to leave fundamental properties of the original equations unaffected: Galilean invariance, conservation of mass and momentum, decay of total kinetic energy for suitable

conditions, and the property that a flow initially at rest at hydrostatic pressure remains unchanged, even if the spatial distribution of volume fractions is nonuniform. The equations with artificial diffusion were proven to have improved stability properties: uniform flow is linearly stable for large wavenumbers, and, in combination with an algebraic drag law, a critical value of the diffusivity exists for which the uniform flow is linearly stable for all wavenumbers. The enhanced stability produced by this artificial diffusivity was confirmed by numerical simulations of the two-phase flow of falling particles in air. A staggered discretization was used, based on central differencing, such that a kinetic energy conserving discretization of convective and volume fraction diffusive terms was obtained. A pressure correction method was presented, using a Poisson equation for multiphase flow. Simulations were performed for uniform and nonuniform mean profiles. The simulations without diffusion term in the volume fraction equation became unstable and could not be completed. However, the simulations with artificial diffusion converged to the steady state solution, at least if the analytically derived stability constraint on the artificial diffusivity was satisfied.

## Appendix 1

Three steps of the analysis in section 3 are further explained in this appendix.

First, we show the derivation of Eq. (30) from Eq. (26). Using the definition of  $\lambda$  (Eq. (27)), Eq. (26) can be written as:

$$\begin{vmatrix} \lambda - u_1 & -\alpha_1 & 0 & 0 \\ -(\lambda - u_2) & 0 & -\alpha_2 & 0 \\ \frac{i\gamma(u_1 - u_2)}{\rho_1 k} & \lambda - u_1 - i(\nu_1 k - \eta k + \frac{\hat{\gamma}\alpha_2}{\rho_1 k}) & \frac{i\hat{\gamma}\alpha_2}{\rho_1 k} & -\frac{1}{\rho_1} \\ \frac{i\gamma(u_1 - u_2)}{\rho_2 k} & \frac{i\hat{\gamma}\alpha_1}{\rho_2 k} & \lambda - u_2 - i(\nu_2 k - \eta k + \frac{\hat{\gamma}\alpha_1}{\rho_2 k}) & -\frac{1}{\rho_2} \end{vmatrix} = 0. \quad (78)$$

Expansion of the determinant along the last column results in

$$\begin{aligned} & \frac{1}{\rho_1} \left[ (\lambda - u_1) \frac{i\hat{\gamma}\alpha_1\alpha_2}{\rho_2 k} - (\lambda - u_2)\alpha_1 \left( (\lambda - u_2) - i(\nu_2 k - \eta k + \frac{\hat{\gamma}\alpha_1}{\rho_2 k}) \right) \right] \\ & - \frac{1}{\rho_2} \left[ (\lambda - u_1)\alpha_2 \left( (\lambda - u_1) - i(\nu_1 k - \eta k + \frac{\hat{\gamma}\alpha_2}{\rho_1 k}) \right) + (\lambda - u_2) \left( -\frac{i\hat{\gamma}\alpha_1\alpha_2}{\rho_1 k} \right) \right] \\ & + \left( \frac{1}{\rho_1\rho_2} - \frac{1}{\rho_2\rho_1} \right) \frac{i\gamma\alpha_1\alpha_2(u_1 - u_2)}{k} = 0. \end{aligned} \quad (79)$$

Multiplication of this equation with  $-\rho_1\rho_2$  gives

$$\begin{aligned} & \alpha_1\rho_2(\lambda - u_2) \left( (\lambda - u_2) - i(\nu_2 - \eta)k \right) - i(\lambda - u_2)(\alpha_1^2 + \alpha_1\alpha_2) \frac{\hat{\gamma}}{k} \\ & + \alpha_2\rho_1(\lambda - u_1) \left( (\lambda - u_1) - i(\nu_1 - \eta)k \right) - i(\lambda - u_1)(\alpha_2^2 + \alpha_1\alpha_2) \frac{\hat{\gamma}}{k} = 0. \end{aligned} \quad (80)$$

After substitution of

$$\alpha_1^2 + \alpha_1\alpha_2 = \alpha_1(\alpha_1 + \alpha_2) = \alpha_1, \quad (81)$$

$$\alpha_2^2 + \alpha_1\alpha_2 = \alpha_2(\alpha_1 + \alpha_2) = \alpha_2, \quad (82)$$

which is valid since  $\alpha_1 + \alpha_2 = 1$ , Eqs. (30-36) can be derived.

Second, we prove the negativity of the growth rate if  $k \rightarrow \infty$  in combination with  $q \rightarrow 0$  and  $|r| \rightarrow \infty$ . This combination may occur if  $\zeta = 0$ . Thus let  $k \rightarrow \infty$ ,  $q \rightarrow 0$  and  $|r| \rightarrow \infty$ . The value of  $y$  cannot converge to zero, since  $y \rightarrow 0$  would imply  $|s| \rightarrow \infty$  because of (38) and then (37) would imply  $|y| \rightarrow \infty$ , a contradiction to  $y \rightarrow 0$ . Since  $y \rightarrow 0$  is not true, (38) implies  $s \rightarrow (by - r)/2ay$ . Substitution of the latter limit into (37) leads to

$$4a^3y^4 + a(b^2 - 4ac)y^2 - ar^2 = 0. \quad (83)$$

Since  $|r| \rightarrow \infty$ , we find

$$|y| \rightarrow (|r|/2a)^{\frac{1}{2}} \sim k^{\frac{1}{2}}, \quad |s| \rightarrow (|r|/2a)^{\frac{1}{2}} \sim k^{\frac{1}{2}}. \quad (84)$$

Then Eq. (27) implies that  $\Omega$  has a negative imaginary part, since  $\eta > 0$  and  $k^{3/2}$  is small compared to  $k^2$  if  $k \rightarrow \infty$ .

Third, we prove Eq. (51). Substitution of the definitions of  $a$ ,  $b$ ,  $c$  and  $w$  into the left-hand side of (51) leads to

$$\begin{aligned} & (\alpha_2\rho_1 + \alpha_1\rho_2)(\alpha_1^2u_2^2 + \alpha_2^2u_1^2 + 2\alpha_1\alpha_2u_1u_2) - 2(\alpha_2\rho_1u_1 + \alpha_1\rho_2u_2)(\alpha_1u_2 + \alpha_2u_1) \\ & + \alpha_2\rho_1u_1^2 + \alpha_1\rho_2u_2^2, \end{aligned} \quad (85)$$

which is equal to

$$u_1^2((\alpha_2^3 - 2\alpha_2^2 + \alpha_2)\rho_1 + \alpha_1\alpha_2^2\rho_2) + u_2^2((\alpha_1^3 - 2\alpha_1^2 + \alpha_1)\rho_2 + \alpha_1^2\alpha_2\rho_1) - 2u_1u_2((\alpha_1\alpha_2 - \alpha_1\alpha_2^2)\rho_1 + (\alpha_1\alpha_2 - \alpha_1^2\alpha_2)\rho_2). \quad (86)$$

After substitution of

$$\begin{aligned} \alpha_2^3 - 2\alpha_2^2 + \alpha_2 &= \alpha_2(\alpha_2 - 1)^2 = \alpha_1^2\alpha_2, \\ \alpha_1^3 - 2\alpha_1^2 + \alpha_1 &= \alpha_1(\alpha_1 - 1)^2 = \alpha_1\alpha_2^2, \\ \alpha_1\alpha_2 - \alpha_1\alpha_2^2 &= \alpha_1\alpha_2(1 - \alpha_2) = \alpha_1^2\alpha_2, \\ \alpha_1\alpha_2 - \alpha_1^2\alpha_2 &= \alpha_1\alpha_2(1 - \alpha_1) = \alpha_1\alpha_2^2, \end{aligned} \quad (87)$$

all valid since  $\alpha_1 + \alpha_2 = 1$ , the right-hand side of Eq. (51) follows.

## Appendix 2

Here the proof is given for the statement in section 5 that reuse of face quantities from the continuity equations in the momentum equations, as it has been proposed in Ref. [5], leads to discrete energy conservation of the convective and volume fraction diffusive terms, if the time integration is exact. Denoting the grid cell with index  $i$  and omitting the phase index, the spatial discretization of the continuity equation and momentum equation per phase in the staggered finite volume method reads:

$$\partial_t \alpha_{i-\frac{1}{2}} = -\frac{1}{h}(f_i - f_{i-1}), \quad (88)$$

$$\partial_t \left( \frac{1}{2}(\alpha_{i-\frac{1}{2}} + \alpha_{i+\frac{1}{2}})u_i \right) = -\frac{1}{4h_i} \left( (u_i + u_{i+1})(f_i + f_{i+1}) - (u_{i-1} + u_i)(f_{i-1} + f_i) \right) + R_i, \quad (89)$$

where  $f$  is the sum of convective and diffusive fluxes through the cell faces in the continuity equation,  $h_i$  is the grid spacing, and  $R_i$  represents all other terms in the momentum equation. In this appendix no summation convention of indices is used. The time derivative of discrete total kinetic energy in the phase under consideration is derived from the two discrete equations above:

$$\begin{aligned} \partial_t \left( \frac{1}{4}(\alpha_{i-\frac{1}{2}} + \alpha_{i+\frac{1}{2}})u_i^2 \right) &= u_i \partial_t \left( \frac{1}{2}(\alpha_{i-\frac{1}{2}} + \alpha_{i+\frac{1}{2}})u_i \right) - \frac{1}{4}u_i^2(\partial_t \alpha_{i-\frac{1}{2}} + \partial_t \alpha_{i+\frac{1}{2}}) \\ &= -\frac{1}{4h_i} \left( u_i(u_i + u_{i+1})(f_i + f_{i+1}) - u_i(u_{i-1} + u_i)(f_{i-1} + f_i) \right. \\ &\quad \left. - u_i^2(f_i - f_{i-1} + f_{i+1} - f_i) \right) + u_i R_i, \\ &= -\frac{1}{4h_i} \left( u_i^2 f_i + u_i^2 f_{i+1} + u_i u_{i+1} f_i + u_i u_{i+1} f_{i+1} - u_{i-1} u_i f_{i-1} \right. \\ &\quad \left. - u_{i-1} u_i f_i - u_i^2 f_{i-1} - u_i^2 f_i + u_i^2 f_{i-1} - u_i^2 f_{i+1} \right) + u_i R_i \\ &= -\frac{1}{4h_i} \left( u_i u_{i+1} f_i - u_{i-1} u_i f_{i-1} + u_i u_{i+1} f_{i+1} - u_{i-1} u_i f_i \right) + u_i R_i. \end{aligned} \quad (90)$$

If we sum over all  $i$  in the domain, multiply with  $h$ , we obtain the time derivative of discrete kinetic energy in the phase under consideration,

$$\begin{aligned}
& \partial_t \sum_i \left( \frac{h_i}{4} (\alpha_{i-\frac{1}{2}} + \alpha_{i+\frac{1}{2}}) u_i^2 \right) \\
&= -\frac{1}{4} \left( \sum_i u_i u_{i+1} f_i - \sum_i u_{i-1} u_i f_{i-1} + \sum_i u_i u_{i+1} f_{i+1} - \sum_i u_{i-1} u_i f_i \right) + \sum_i h_i u_i R_i \\
&= -\frac{1}{4} \left( \sum_i u_i u_{i+1} f_i - \sum_i u_i u_{i+1} f_i + \sum_i u_i u_{i+1} f_{i+1} - \sum_i u_i u_{i+1} f_{i+1} \right) + \sum_i h_i u_i R_i \\
&= \sum_i h_i u_i R_i. \tag{91}
\end{aligned}$$

where the shift of the index of the sums is justified by the assumption of periodic boundary conditions. This equation shows that the discrete convective and volume fraction diffusive terms do not contribute to the time derivative of total kinetic energy.

## References

- [1] T.B. Anderson, R. Jackson, A fluid mechanical description of fluidized beds, IEC Fundamentals 6 (1967) 527-539.
- [2] M. Arai, Characteristics and stability analysis for two-phase flow equation systems with viscous terms, Nucl. Sci. Eng. 74 (1980) 77-83.
- [3] M.R. Baer, J.W. Nunziato, A two-phase mixture theory for the deflagration-to-detonation transition (DDT) in reactive granular materials, Int. J. Multiphase Flow 12 (1986) 861-889.
- [4] J.B. Bdzil, R. Menikoff, S.F. Son, A.K. Kapila and D.S. Stewart, Two-phase modeling of deflagration-to-detonation transition in granular materials: A critical examination of modeling issues, Phys. Fluids 11 (1999) 378-402.
- [5] B.J. Boersma, A staggered compact finite difference formulation for the compressible Navier-Stokes equations, J. Comp. Physics 208 (2005) 675-690.
- [6] C. Crowe, M. Sommerfeld, M. Tsuji, Multiphase flows with droplets and particles, CRC Press LLC, Boston, 1998.
- [7] D.A. Drew, Mathematical modeling of two-phase flow, Ann. Rev. Fluid Mech. 15 (1983) 261-291.
- [8] D.A. Drew, A turbulent dispersion model for particles or bubbles, J. Eng. Math. 41 (2001) 259-274.
- [9] D.A. Drew, S.L. Passman, Theory of multicomponent fluids, Springer, New York, 1998.
- [10] S.E. Elghobashi, T.W. Abou-Arab, A two-equation turbulence model for two-phase flows, Phys. Fluids 26 (1983) 931-938.
- [11] F.E. Harlow, J.E. Welsh, Numerical calculation of time-dependent viscous incompressible flow of fluid with free surface, Phys. Fluids 8 (1965) 2182.

- [12] H. Holmas, T. Sira, M. Nordsveen, H.P. Langtangen, R. Schulkes, Analysis of a 1D incompressible two-fluid model including artificial diffusion, *IMA J. Appl. Math.* 73 (2008), 651-667.
- [13] M. Ishii, *Thermo-fluid dynamic theory of two-phase flow*, Eyrolles, 1975.
- [14] R.I. Issa, P.J. Oliveira, Modeling of turbulent dispersion in two phase flow jets, *Engineering Turbulence Modeling and Experiments 2*, W. Rodi and F. Martelli (Editors) (1993), 947-957.
- [15] R.I. Issa, M.H.W. Kempf, Simulation of slug flow in horizontal and nearly horizontal pipes with the two-fluid model, *Int. J. Multiphase Flow* 29 (2003), 69-95.
- [16] R. Jackson, *The dynamics of fluidized particles*, Cambridge University Press, 2000.
- [17] A. Jameson, *Transonic Flow Calculations*, Princeton University Report MAE 1651, March 1984, in *Numerical Methods in Fluid Dynamics*, edited by F. Brezzi, *Lecture Notes in Mathematics*, Vol. 1127, Springer-Verlag, 1985, pp. 156-242.
- [18] A.V. Jones, A. Prosperetti, On the suitability of first-order differential models for two-phase flow prediction, *Int. J. Multiphase Flow* 11 (1985) 133-148.
- [19] C. Laborde-Boutet, F. Larachi, N. Dromard, O. Delsart, D. Schweich, CFD simulation of bubble column flows: Investigations on turbulence models in RANS approach, *Chemical Engineering Science* 64 (2009) 4399-4413.
- [20] D. Lucas, E. Krepper, H.M. Prasser, Use of models for lift, wall and turbulent dispersion forces acting on bubbles for poly-disperse flows, *Chemical Engineering Science* 62 (2007), 4146-4157.
- [21] R.W. Lyczkowski, D. Gidaspow, C.W. Solbrig, E.C. Hughes, Characteristics and stability analysis of transient one-dimensional two-phase flow equations and their finite difference approximations, *ASME Meeting*, Houston (1975).
- [22] A. Michalke, On the inviscid instability of the hyperbolic-tangent velocity profile, *J. Fluid Mech.* 19 (1964) 543-556.
- [23] R.S. Oey, R.F. Mudde, L.M. Portela, H.E.A. van den Akker, Simulation of a slurry airlift using a two-fluid model, *Chemical Engineering Science* 56 (2001) 673-681.
- [24] H. Pokharna, M. Mori, V.H. Ransom, Regularization of two-phase flow models: a comparison of numerical and differential approaches, *J. Comp. Physics* 134 (1997), 282-295.
- [25] J.M. Powers, Two-phase viscous modeling of compaction of granular materials, *Phys. Fluids* 16 (2004), 2975-2990.
- [26] A. Prosperetti, A.V. Jones, The linear stability of general two-phase flow models - II, *Int. J. Multiphase Flow*, 13 (1987) 161-171.
- [27] A. Prosperetti, G. Tryggvason, *Computational Methods for multiphase flow*, Cambridge University Press, 2006.
- [28] J.D. Ramshaw, Brownian motion in multiphase flow, *Theor. Comp. Fluid Dyn.* 14 (2000) 195-202.

- [29] J.D. Ramshaw, J.A. Trapp, Characteristics, stability, and short-wavelength phenomena in two-phase flow equation systems, *Nucl. Sci. Eng.* 66 (1978) 93-102.
- [30] M. Syamlal, T.J. O'Brien, Computer simulation of bubbles in a fluidized bed. *A.I.Ch.E. Symposium Series* 85 (1989) 22-31.
- [31] F. Taghipour, N. Ellis, C. Wong, Experimental and computational study of gas-solid fluidized bed hydrodynamics, *Chemical Engineering Science* 60 (2005) 6857-6867.
- [32] M.A. van der Hoef, M. van Sint Annaland, N.G. Deen, J.A.M. Kuipers, Numerical simulation of dense gas-solid fluidized beds: a multiscale modeling strategy, *Ann. Rev. Fluid Mech.* 40 (2008) 47-70.
- [33] R.W.C.P. Verstappen, A.E.P. Veldman, Symmetry-preserving discretization of turbulent flow, *J. Comp. Physics* 187 (2003) 343-368.
- [34] A.W. Vreman, Macroscopic theory of multicomponent flows: irreversibility and well-posed equations *Physica D: Nonlinear phenomena* 225 (2007) 94-111.
- [35] P. Wesseling, *Principles of computational fluid dynamics*, Springer, Berlin, 2000.
- [36] G.B. Whitham, *Linear and nonlinear waves*, John Wiley & Sons, New York, 1974.